Praise Worthy Prize

This paper is available online at www.praiseworthyprize.org
International Review on Modelling and Simulations (I.RE.MO.S.), Vol. 15, N. 6
ISSN 1974-9821
December 2022

The Wing Structure of an F3J/F5J Competition Sailplane: Topological Optimisation with Simplex Method and Additive Manufacturing

E. Seminara, G. Laudani, G. Baiamonte, M. Calì

Abstract – *This research concerns the optimization study of the wing of an ultralight competition sailplane, category F5J/F3J. Fundamental for this category is the characteristic of lightness associated with good wing stiffness (bending/torsional). All the elements composing the wing of the sailplane were modelled in 3D by using the Autodesk Inventor parametric solid modeler. They were assembled in the FEM environment and were suitably constrained and studied from a structural point of view. The structural characteristics of the wing and its components were analysed in detail after assigning the materials currently used and adopting appropriate materials to make the same with the Additive Manufacturing (AM) technic. A topological optimization, performed by using the Simplex Method (SIMP), was conducted on the internal structure of the wing in order to lighten the ribs with the same performance. The experimental investigations implemented in the laboratory allowed the 'Oralight' material used for the wing surface coating to be characterized. It is an extremely thin and light material, whose elasticity and strength were accurately assessed in this study. The data obtained, considered along with the elasticity and the resistance values of the other materials constituting the wing structure, taken from the literature, were inserted into the finite element simulations with the aim of evaluating the torsional and bending stiffness of the wing. Finally, the rib was redesigned using a FDM material which makes construction particularly simple.* ***Copyright © 2022 The Authors.***

Keywords: *Wing Parametric Modelling, "Oralight" Coating Surface, Ribs and Spars' Redesign, Compound Bio-Plastic Filament, Torsional and Bending Wing Stiffness*

Nomenclature

ρ	Density
CL	Aerodynamic coefficient
K_B	Bending stiffness
K_T	Torsional stiffness
L	Effective lift
S	Wing surface
v	Flight speed

I. Introduction

Since the beginning of the last century, there has been growing interest in the design of high-performance gliders [1], as they are an example of sustainable engineering in aeronautics. A sailplane is an aerodine, i.e. an aircraft heavier than air, supported in flight by the dynamic response of the air against the wing surfaces; it does not necessarily require an engine to fly. Mainly used for sport, this sailplane can be also employed for scientific studies and military purposes [2]-[4]. To be efficient, airfoil design procedures require a fast and robust analysis method with which the performance can be evaluated both in and out of the design phase. In particular, the wing of a glider must be designed to conform to specified mission and design requirements.

High aerodynamic efficiency and good stall characteristics are some of the design requirements, while achieving level flight at a particular altitude may be a mission requirement [5]. Of the various airfoil analysis algorithms developed to date, only an integrated approach characterized by finite element models allows to produce a fast and reliable design of structurally and aerodynamically optimised airfoils. In particular, the formulation of an interactive fluid-dynamic-structural analysis enables the designer to optimise a glider performance by the choice of structure topology; flexible multi-body dynamics with floating reference system formulation is applied to analyse system behaviour during motion in high and low speed configurations [6].

In this research, the problem concerning a topological optimisation of the structures (ribs and spars) of the wing of an ultra-light glider was addressed. In particular, by applying a solid-parametric modelling procedure performed with the commercial software Inventor 2022 and a structural analysis with the commercial finite-element code Ansys 2020 R2, the wing profiles of the 'Bubble Dancer' glider were optimised in terms of stiffness and weight. Procedures similar to the one used here have been used by the authors in many of their

Available online by December 31st, 2022
https://doi.org/10.15866/iremos.v15i6.23066

recent works. [7]-[10]. This sailplane is usually constructed from balsa, carbon fibre and epoxy resin composites and Oralight (or similar). Equipped with a wingspan of 3 m and a wing surface area of 0.645 m^2, it was designed and optimized by the American Aeronautical Engineer Mark Drela, Professor of Fluid Dynamics at the Massachusetts Institute of Technology (MIT) [11], [12]. The aim of the present research was to create a large model based on thermal flight that anyone could build, able to tolerate substantial aerodynamic loads. With a take-off weight of 880 gr, it had a very low sink rate of about 0.25 m/s. A very large 50 mm × 915 mm spoiler that offered a good landing control, and can be seen taking flight very often by hand or winch launches, withstanding high thrusts compared to common models of similar size [13].

The research work that is presented here followed these steps. Section II deals with the design of the sailplane's aerodynamic structure. Section III shows the experimental characterization of the "Oralight" coating surface; it was performed by tensile tests with Istron 6800 Series. Section IV describes the torsional, bending and displacement analysis of the skeleton and the complete wing structure. Section V deals with the topological optimisation and structural analysis, implemented by using 3D modelling and the Finite Element Method. In Section VI the printing of the topologically optimised rib' structure, through FDM with a new compound bio-plastic filament HEMP, is described. Finally, in Section VII and in Section VIII the discussions and the conclusions are drawn, respectively.

II. Design of Sailplane Aerodynamic Structures

The 'structure' comprises what binds the parts of the aircraft together (such as the wings) which create the lift, the fuselage, which is designed to store the 'payload' and connect the wings to the tail planes, the aerodynamic control elements (wings and tail planes), the propulsion system and the landing gear. Mainly, three types of structures can be distinguished: frame structures, shell structures and half-shell structures; all of them are used in aviation, sometimes together. A trellis construction consists of wooden or metal trusses that are then covered, often with canvas. The metal frame absorbs all the stresses in the lattice structure, leaving the cladding the main role of creating the aerodynamic load. The cladding, on the other hand, is an integral part of the shell structure and serves to absorb stresses; Particularly, the shell must meet certain requirements, so that it adopts the desired aerodynamic shape even between the ribs that impose its deformation [14]. Although the halfshell structure is a shell construction, but it is possible to identify certain components (the longitudinal members, the spars) that provide bending resistance, while the cladding is simply left to react to torsional loads. The early aircrafts were designed with 'lattice' constructions which were often made of wood and covered with canvas. However, this approach proved to be inadequate for high speeds, so aircraft was built with metal cladding, in particular aluminium considered its low weight and mechanical properties far superior to canvas and even the same wood used for the internal structure, which was soon made of aluminium [15]. The fabric usually adopted for covering the 'Oralight' wings was characterised experimentally by tensile strength performing five tests on specially prepared unified specimens, ASTM D 882 standard (Fig. 1).

III. Coating Surface's Experimental Characterization

To characterize the "Oralight" coating surface, the tests were performed by using the Instron 6800 Series tensile testing machine (Fig. 2), setting the following test parameters: - Preload = 1 N - Traslational velocity = 20 mm/s. The lower part of the test specimen was clamped in the fixed cross beam of the machine, while the upper part of the test specimen was clamped in the movable cross beam of the machine. A strain gauge was assembled with the following data plate during the test run. The two terminals of the strain gauge were connected to the central part of the test specimen, the useful part, i.e. the area subject to elongation. For all the test specimens, it was mounted at the start of each test in order to validate their reliability and to make the measurement independent of any displacement of the specimen with respect to the moving crosshead. When this displacement coincided with that read by the strain gauge, no slippage was registered and the test could be considered reliable [16], [17].

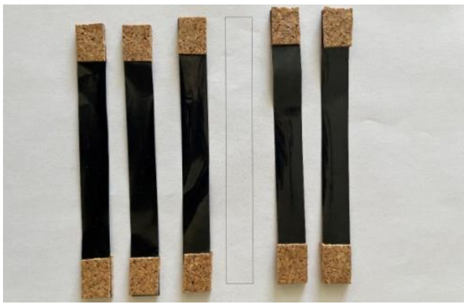

Fig. 1. Oralight specimens (ASTM D 882)

Fig. 2. Oralight specimens' tests in Instron 6800

The tests performed in this study made it possible to assess the Young's (elastic) modulus of the material (Fig. 3), the extent of the elastic zone and the values of the yield; fracture stresses of the material were also evaluated [18], [19]. The calculated values permitted to implement particularly realistic finite element simulations. The final wing solid-parametric model can be seen in Figs. 4 and 5.

IV. Wing's Torsional and Bending Stiffness Evaluation

Finited Element Method (FEM) is widely used in the engineering field for the analysis of complex structures by representing them through partial derivative equations via domains that correspond to the shapes of the object under investigation. Torsion and bending studies were conducted on the wing 'skeleton' consisting of ribs and spar components and on the wing complete with covers and cladding. In the tests performed, the forces and moments were applied to the wing's tip panel, with the results reported for each of them.

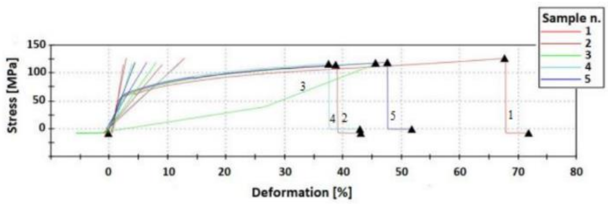

Fig. 3. Unified test specimens' results, ASTM D 882 standard

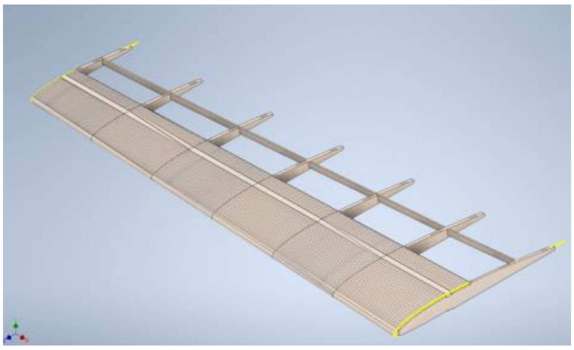

Fig. 4. Extremities of F3J/F5J wing structure

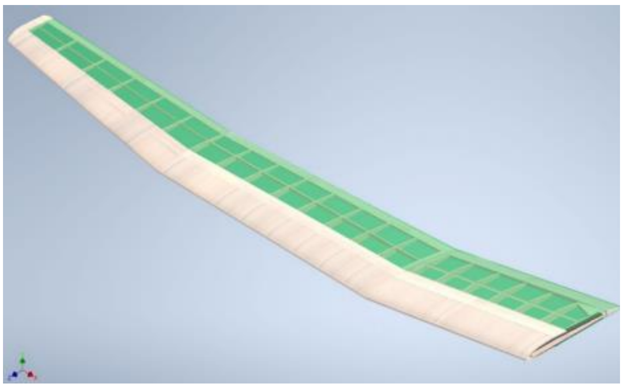

Fig. 5. Complete F3J/F5J wing structure

It is important to specify that the scale of the graphical representation did not represent the values of the actual measurements found by the FEM studies, but it was amplified in order to better show the displacements that the structure underwent.

The torsional analysis was performed by applying a moment equal to 1 Nm on the external face of the last rib of the wing tip panel (Fig. 6).

The maximum value obtained regarding the von Mises stress was 28.51 MPa. It was possible to calculate the torsional stiffness as:

$$K_T = \frac{\text{Applied moment}}{\text{Angle of rotation}} = \frac{10\ \text{Nm}}{1{,}529°} = 0{,}654\ \text{Nm} \qquad (1)$$

This equation made it possible to assess the relative rotation between the wing extremities and thus to calculate the torsional stiffness of the structure. The maximum structure's relative displacement was 1.321 mm (Fig. 7).

The bending analysis was conducted by applying a force of 10 N on the lower face of the last rib of the wing tip panel, the one corresponding to the transition and support area of the spar reinforcement. To avoid high stress concentrations the force of 10 N was applied to an area of approximately 2 cm^2 (Fig. 8(a)).

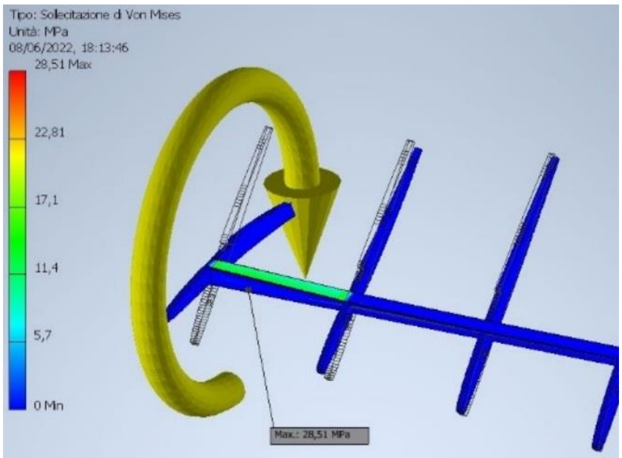

Fig. 6. Wing skeleton details, max. von Mises stress, moment: 1 Nm

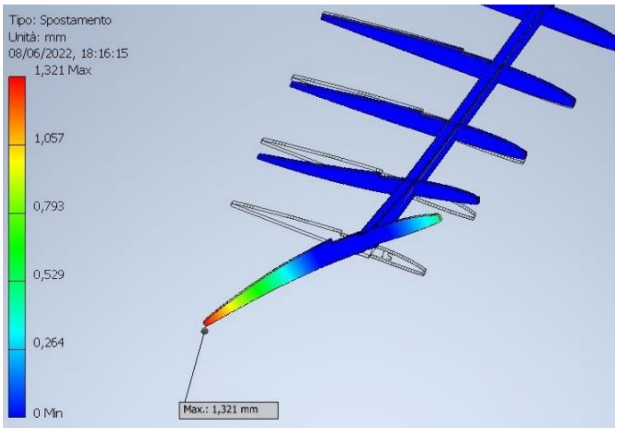

Fig. 7. Max wing skeleton displacement, moment: 1 Nm

In this configuration a maximum displacement of 0.1345 mm was rated (Fig. 8(a)). Therefore, the wing bending stiffness was calculated as:

$$K_F = \frac{\text{Applied force}}{\text{Total desplacement}} = \\ = \frac{10\ \text{N}}{0{,}1345\ \text{mm}} = 74{,}349\frac{\text{N}}{\text{mm}} \quad (2)$$

The torsional analysis was conducted by applying a moment equal to 1 Nm to the external face of the last rib of the wing tip panel (Fig. 9). As for the structure displacement analysis, the maximum value found corresponded to 1.626 mm. The torsional stiffness factor was calculated as:

$$K_T = \frac{\text{Applied moment}}{\text{Angle of rotation}} = \frac{1\ \text{Nm}}{1{,}242°} = 0{,}805\ \text{Nm} \quad (3)$$

The bending analysis was conducted by applying a pressure of 13.3 MPa distributed on the lower face of the wing's bottom spar reinforcement (Fig. 10). The choice of this pressure value was made to obtain a stress comparable to that of the previous case, without having stress concentrations on very small surfaces (use of concentrated forces).

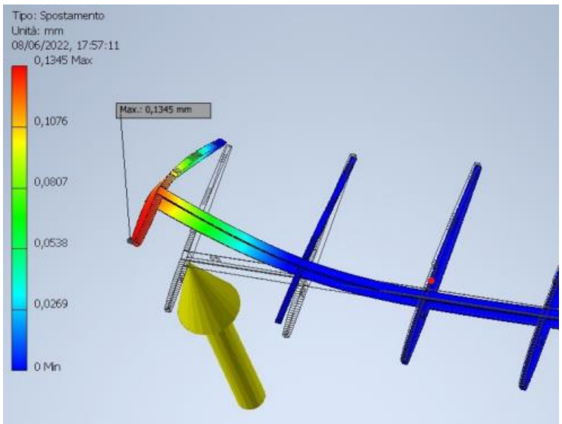

(a)

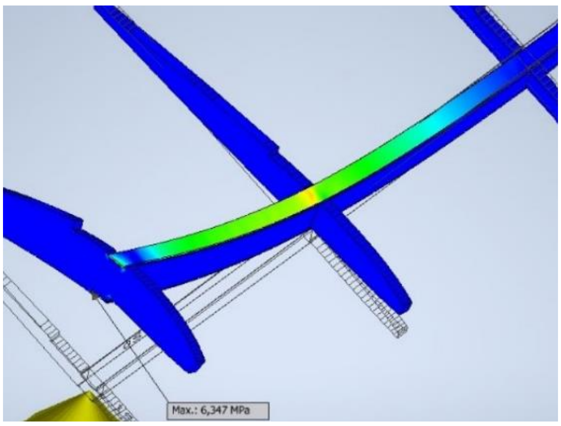

(b)

Figs. 8. (a) Max. wing skeleton displacement, force: 10 N; (b) Max. wing skeleton von Mises stress, force: 10 N

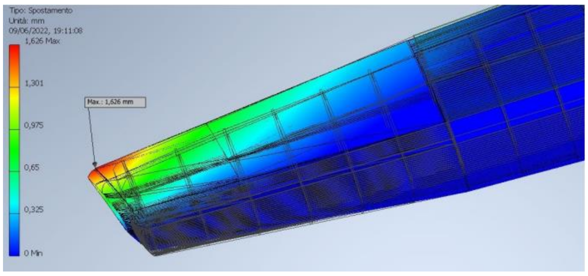

Fig. 9. Max. displacement of complete wing structure, moment: 1 Nm

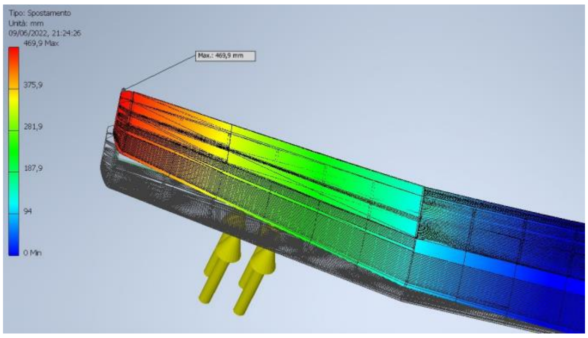

Fig. 10. Max. displacement of complete wing structure, pressure: 13.3 MPa

When analysing the displacements of the structure, the maximum value found corresponded to 469.9 mm (Fig. 10). The bending stiffness was calculated as:

$$K_B = \frac{\text{Applied force}}{\text{Total desplacement}} = \\ = \frac{37340\ \text{N}}{469{,}9\ \text{mm}} = 79{,}562\frac{\text{N}}{\text{mm}} \quad (4)$$

V. Topological Optimisation and Structural Analysis

The topological optimisation for the sailplane's structure was obtained by using the Solid Isotropic Material with Penalisation (SIMP) method. Specifically, it was achieved by defining an appropriate initial geometry, which considered all the geometric and structural constraints, and applying real static and dynamic loads. In this way, a complete and multiload dynamic model provided all necessary dynamic data. In addition, it allowed the optimisation results obtained to be verified [20], [21]. The topological optimisation method so applied was divided into several steps that can be resumed hereafter:

- Input optimisation: 3D CAD model with the appropriate forces and constraints that the part had to withstand once in the operation assigned;
- The areas of the part that must not be processed or altered, such as fixtures, assembly holes or other elements vital for the part to function properly, were defined (e.g. if the part has an assembly hole in it, that area will be excluded from the optimisation process);
- FEM analyses were performed cyclically on the

object, allowing its structural behaviour to be calculated;

- The programme reduced the percentage of the material that is not requested to maintain the safety requirements set on the basis of the previous FEM analyses performed (as well as possibly involving the production technique for which the optimisation is applied);
- Optimisation output: the optimised part obtained through the various processes was lighter than the initial one and continued to meet the desired mechanical requirements [22]-[24]. The structural analysis started by using the ANSYS software [25]-[27], by setting values of mesh resolution in the following way:
  - Resolution = 7;
  - Transition = Slow;
  - Span Angle Centre = Fine;
  - Smoothing = High.

After resolution, two values of pressures were inserted to simulate the effect of lift, acting one on the lower face and one on the upper face of the rib. These pressures were calculated on the basis of the design data concerning the maximum stresses that the sailplane can sustain with regard to the lift on the wing structure. In order to work with a fairly wide safety margin, a situation of 166 % of the critical design situation was examined. Considering an aerodynamic coefficient *CL* = 1, these design loads resulted in a maximum lift value of 667.23 N at a flight speed of 40.23 m/s; the tests were therefore performed considering a flight speed of 67.06 m/s (150 mph) and the effective lift was calculated using the following relationship:

$$L = CL \times \left(\frac{1}{2}\right) \times \rho \times v^2 \times S = 900{,}73 \text{ N} \quad (5)$$

Theoretically, the distribution of lift would be considered as elliptical along the wingspan. For simplicity of calculation and using values far in excess of the conditions of structural safety under maximum stress conditions, it was decided to divide the previously calculated values over the total number of ribs present on the wing, in order to distribute the lift value found approximately over them, and to estimate the force acting on a single rib:

$$\frac{900{,}73 \text{ N}}{21 \text{ ribs}} = 49{,}89 \left[\frac{\text{N}}{\text{rib}}\right] \quad (6)$$

Making a similar approximation, the sum of the surface area of the bases of all the ribs constituting the wing was calculated. For the modelling phase, a value of 0.01533 m^2 was obtained, which was divided by the number of ribs, resulting in an average surface area of 0.00073 m^2/rib. Dividing the value first found by the surface area just calculated:

$$\frac{49{,}89 \left[\frac{\text{N}}{\text{rib}}\right]}{0{,}00073 \left[\frac{\text{m}^2}{\text{rib}}\right]} = 68.342{,}5 \left[\frac{\text{N}}{\text{m}^2}\right] \quad (7)$$

Taking the value 1 atm = 0.1 MPa, and using this as the value for the pressure applied to the upper face of the rib, for the lower face the value of 0.1 + 0.0683 = 0.1683 MPa can be used. Following this return analysis, a topological optimisation was performed. Figure 11 shows the result of the topological optimization for the central rib (Rib 11) of the wing structure. For the other 20 ribs of the structure, the SIMP algorithm provided homologos lightened geometry with 11 oblong holes. Five oblong holes are in correspondence with the leading edge of the wing and six oblong holes in the central part of the ribs.

Below are the graphs of the iteration of the optimisation process and the convergence responses of the algorithm in the calculation of tensile, bending and torsional stresses, respectively (Figs. 12-14).

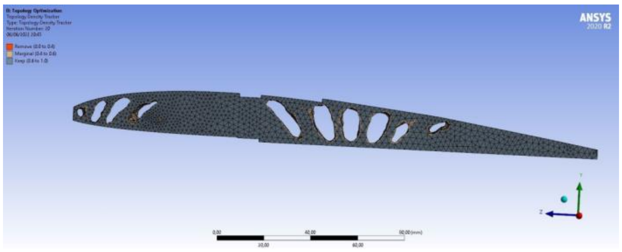

Fig. 11. Result of Topological optimisation for the central rib

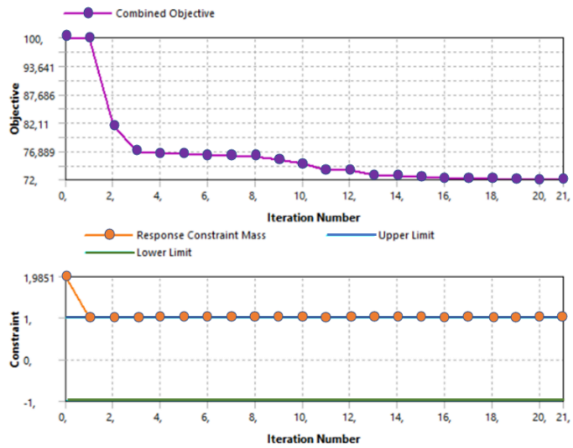

(a)

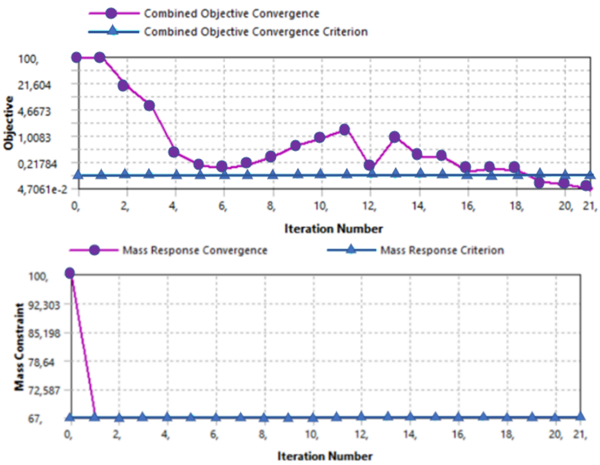

(b)

Figs. 12. Objective & Mass Response Convergence in tensile analysis

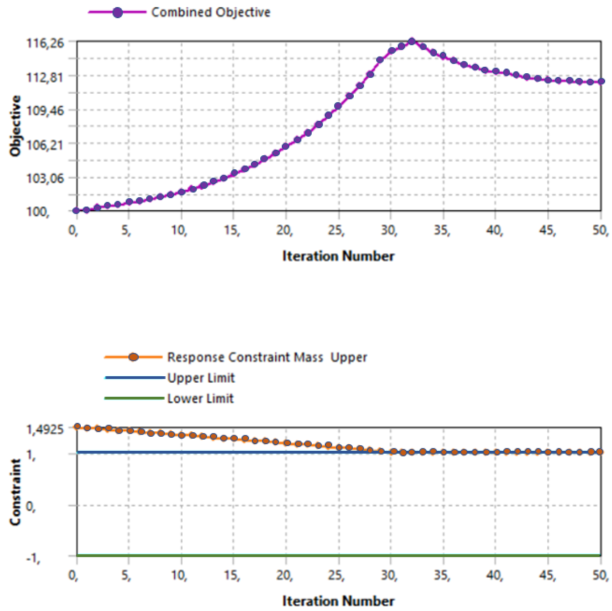

Fig. 13. Objective & Mass Response Convergence in bending analysis

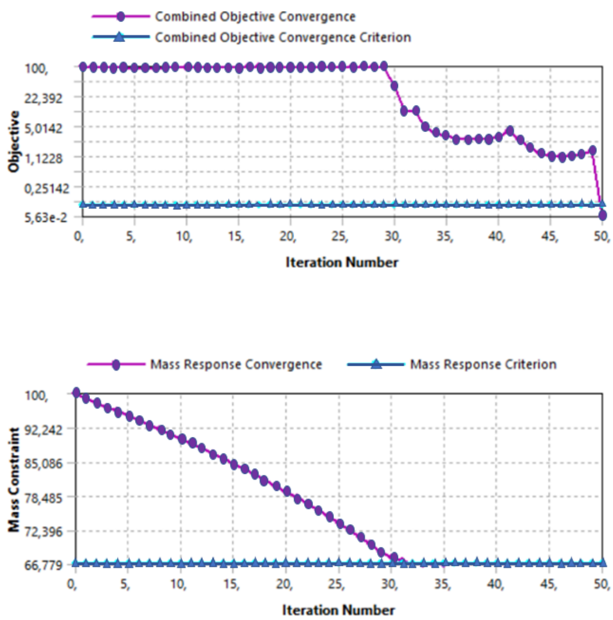

Fig. 14. Objective & Mass Response Convergence in torsional analysis

Through FEM analysis, an equivalent Von Mises stress was obtained with a maximum value of 8.8514 MPa and a minimum of 0.006480 MPa.

VI. Rib's Manufacturing with the New Compounds Bio-Plastic Filament HEMP

To improve the production of the topologically optimised rib, the use of a specific filament, developed by the authors in previous research works [28], [29], was envisaged. In recent years, continuous fibre-reinforced polymer matrix composites have become one of the most promising and basic material groups in many areas of engineering, particularly in the automotive and aerospace industries [30]; Such biopolymer composites have been developed by researchers to provide environmentally responsible materials and thus reduce the carbon footprint. Modification or functionalisation of natural fibres is important to improve interfacial bonding with biopolymers and to obtain high-performance composite materials that can compete with conventional composites based on petrochemical polymers [31]. Biopolymers, indeed, have exceptional mechanical properties with a unique combination of strength and toughness, as well as biological functions that interact with their environment [32]. In particular, a filament of bio-plastic composite of natural origin and compostable containing hemp (with a percentage of 15%) was used, which was named HEMP by the authors. Compared to common composite materials, this compound was entirely natural-based. The matrix consists of Polylactic Acid (PLA), a 100 % bio-based plastic (purchased from NatureWorks' Ingeo Biopolymer 3D450), while the reinforcement consisted of particles (more than 20 % by weight) from hemp waste. In particular, HEMP provided a performance in terms of lightness, strength and roughness, making it suitable for rib printing. This material also can reduce the cost of environmental impact and production management costs. Figures 15 show the stress state (Fig. 15(a)) and the deformation state (Fig. 15(b)) obtained on the central rib topologically optimized, built by using the HEMP printing filament. Note that the ribs on average presented stresses and deformations only slightly higher than the original ones, while the wing structure presented an overall weight reduction of about 20% compared to the initial geometry built in balsa wood. The material used would also allow small benefits to be achieved in the non-topologically optimised structure.

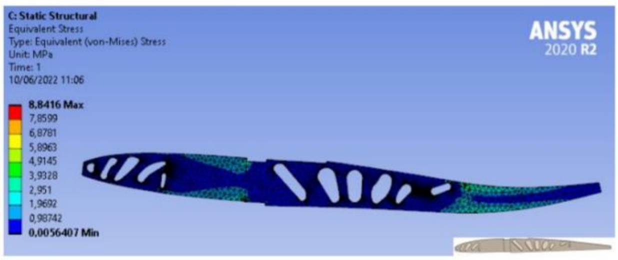

(a)

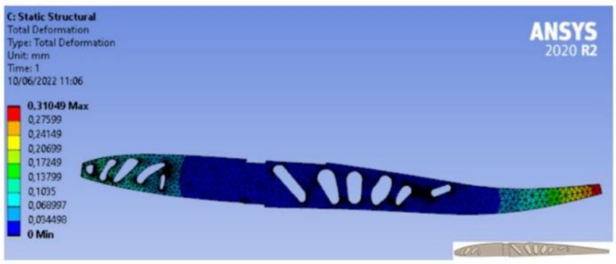

(b)

Figs. 15. Finite element analyses of Rib topologically optimised structure printed with HEMP: (a) Stress, (b) Deformation

VII. Discussion

The SIMP method applied to the F3J/F5J competition sailplane structure allowed to obtain interesting results for the ribs topological optimisation process. The percentage of the unnecessary material was reduced by 20%, while maintaining the established safety requirements. As a result, the obtained part was lightened, thus reducing the aerodynamic drag; this allowed the entire aircraft to support itself more easily in flight and achieve higher aerodynamic efficiency values between aircraft and wing for long distances and high speeds.

VIII. Conclusion

In this reserch the optimisation problem of the wing structure of an ultralight sailplane was addressed, advancing the possibility of using additive manufacturing methods for the construction of the rib parts of the structure. Using the Autodesk Inventor parametric solid modeller, all the components of the wing structure were modelled, and a discretized model of the structure was constructed to verify its possible construction with biopolymer materials (HEMP) other than those currently used (balsa wood and carbon fibre). The results obtained from the experimental tensile characterisation tests evaluated the elasticity and strength characteristics of the materials that make up the cladding surface. In particular, the structure of the fabric covering the wing was characterised. The characterisation of the materials made it possible to accurately assess the torsional and flexural stiffnesses of the wing structure. Finally, a topological optimisation with ANSYS was performed with the aim to evaluated the use of FDM techniques to construct the ribs with a new plastic filament compound (HEMP). For the future, we intend to further study biopolymer materials applications with the aim to improve the mechanical rib properties and significantly reduce their weight. In this way, the main goal could will become the application of this type of material to construct the entire sailplane structure; in this way the important benefit of reducing environmental impact could will be obtained too.

References

[1] Seeni, A. (2021). Aerodynamic Analysis and Optimization of Wings for the Jain University Sailplane using XFLR5. *SPAST Abstracts*, 1(01).

[2] Bouskela, A., Chandra, A., Thangavelautham, J., & Shkarayev, S. (2019). *Attitude Control of an Inflatable Sailplane for Mars Exploration*. arXiv preprint arXiv:1902.02083.

[3] Sturm, F., Achleitner, J., Jocham, K., & Hornung, M. (2019). Studies of anisotropic wing shell concepts for a sailplane with a morphing forward wing section. *AIAA Aviation 2019 Forum* (p. 2817).

[4] Hitzel, S. M. (2015, September). Flightphysical aspects and methods of future military aircraft designs. Paper presented In *5th Challenges in European Aerospace CEAS Air & Space Conference* (pp. 1-25).

[5] Kakade, S., Chikkala, D., Reghunath, K., & Seeni, A. (2022). Aerodynamic Analysis and Optimization of Wings for the Jain University Sailplane Using XFLR5. *ECS Transactions*, 107(1) 493.

[6] Gufler, V., Wehrle, E., Achleitner, J., & Vidoni, R. (2021). Flexible multibody dynamics and sensitivity analysis in the design of a morphing leading edge for high-performance sailplanes. In *ECCOMAS Thematic Conference on Multibody Dynamics* (pp. 90-101). Budapest University of Technology and Economics.

[7] Calì, M., Cucinotta, F., Raffaele, M., Salmeri, F., & Sfravara, F. (2023). Voronoi Tessellation Application for Controlling Frequency Domain of a Titanium Plate. In *Flexible Automation and Intelligent Manufacturing: The Human-Data-Technology Nexus: Proceedings of FAIM 2022*, June 19–23, 2022, Detroit, Michigan, USA, Vol. 2 (pp. 125-132). Cham: Springer International Publishing.

[8] Ambu, R., & Calì, M. (2022). Assessment of High Porosity Lattice Structures for Lightweight Applications. In *Flexible Automation and Intelligent Manufacturing: The Human-Data-Technology Nexus: Proceedings of FAIM 2022*, June 19–23, 2022, Detroit, Michigan, USA (pp. 15-26). Cham: Springer International Publishing.

[9] Calì, M., Hajji, B., Nitto, G., & Acri, A. (2022). The Design Value for Recycling End-of-Life Photovoltaic Panels. *Applied Sciences*, 12(18), 9092.

[10] Calì, M., & Ambu, R. (2022). A mesh morphing computational method for geometry optimization of assembled mechanical systems with flexible components. *International Journal on Interactive Design and Manufacturing (IJIDeM)*, 16(2), 575-582.

[11] Drela, M. (1989). XFOIL: An analysis and design system for low Reynolds number airfoils. In *Low Reynolds number aerodynamics* (pp. 1-12). Springer, Berlin, Heidelberg

[12] Drela, M. (2014). *Flight vehicle aerodynamics*. MIT press

[13] Rozov, V.; Volmering, A.; Hermanutz, A.; Hornung, M.; Breitsamter, C. (2019). CFD- Based Aeroelastic Sensitivity Study of a Low-Speed Flutter Demonstrator. *Aerospace*, 6, 30. doi: https://doi.org/10.3390/aerospace6030030

[14] Sturm, F., & Hornung, M. (2021, July). Morphing Shell Design of a Sailplane with a Morphing Forward Wing Section. In *XXXIV OSTIV CONGRESS* (p. 109).

[15] Thesis by Daniele Suraci, UniPd, (a.a 2014/2015), supervisor Prof. Ugo Galvanetto, *Dimensioning the wooden fuselage of an ultralightaircraft*. https://thesis.unipd.it/bitstream/20.500.12608/19403/1/Thesis' Suraci Daniele.pdf

[16] Smith, William F.; Hashemi, Javad, (2006). *Foundations of Materials Science and Engineering* (4ª ed.) McGraw-Hill. ISBN 0-07-295358-6. p. 333.

[17] Callister, William D., Jr., 1940-, *Materials science and engineering: an introduction*, 7th ed, John Wiley & Sons, (2007), ISBN 0471736961, OCLC 61463872.

[18] William D. Callister, (1999*). Material Science and Engineering: An Introduction*, 5ª ed., Master's Thesis, John Wiley & Sons Inc, ISBN 0-471-35243-8.

[19] https://www.oracover.de/film/oralight/1

[20] Orme, M, Madera I, Gschweitl, M, Ferrari, M. Topology Optimization for Additive Manufacturing as an Enabler for Light Weight Flight Hardware. *Designs*. (2018); 2(4):51. doi: https://doi.org/10.3390/designs204005

[21] Calì, M., Oliveri, S., Application of an Effective SIMP Method with Filtering for Topology Optimization of Motorcycle Tubular Frame, (2017) *International Review of Mechanical Engineering (IREME)*, 11 (11), pp. 836-844. doi: https://doi.org/10.15866/ireme.v11i11.13770

[22] Berkovitz, L. D. (2013). *Optimal control theory* Vol. 12. Springer Science & Business Media

[23] Chiandussi, G. (2017). *Optimisation methods applied to engineering problems, Introduction to optimisation methods*.

[24] Sehlström, A., (2013). *Multiobjective topology optimization: Tracing of Pareto- optimal structures with respect to volume, compliance and fundamental eigenvalue* (Master's thesis).

[25] Gunwant, D., & Misra, A., (2012). Topology Optimization of sheet metal brackets using ANSYS. *MIT International Journal of Mechanical Engineering*, 2(2), 120- 126

[26] Tyflopoulos E, Steinert M., (2022). A Comparative Study of the Application of Different Commercial Software for Topology

Optimization. *Applied Sciences*; 12(2):611.
doi: https://doi.org/10.3390/app12020611 (IMG)

[27] Cuellar Loyola, Nilton Alejandro & Pereira, Anderson & Menezes, Ivan., (2015). Robust Topology Optimization Under Uncertain Loads: A Spectral Stochastic Approach. *CILAMCE 2015*.
doi: 10.20906/CPS/CILAMCE2015- 0882

[28] Calì, M., Pascoletti, G., Gaeta, M., Milazzo, Ambu, R. (2020). New filaments with natural fillers for FDM 3D printing and their applications in biomedical field, *Procedia Manufacturing*, Volume 51, Pages 698- 703, ISSN 2351-9789.

[29] Calì, M, Pascoletti, G, Gaeta, M, Milazzo, G, Ambu, R. (2020). A New Generation of Bio-Composite Thermoplastic Filaments for a More Sustainable Design of Parts Manufactured by FDM. *Applied Sciences*;10(17):5852.
doi: https://doi.org/10.3390/app10175852

[30] Trzepieciński T, Najm SM, Sbayti M, Belhadjsalah H, Szpunar M, Lemu HG, (2021). New Advances and Future Possibilities in Forming Technology of Hybrid Metal–Polymer Composites Used in Aerospace Applications. *Journal of Composites Science*; 5(8):217.
doi: https://doi.org/10.3390/jcs5080217

[31] Aaliya, B., Sunooj, K. V., & Lackner, M. (2021). Biopolymer composites: A review. *International Journal of Biobased Plastics*, 3(1), 40-84

[32] Ling, S., Chen, W., Fan, Y., Zheng, K., Jin, K., Yu, H., ... & Kaplan, D. L. (2018). Biopolymer nanofibrils: Structure, modeling, preparation, and applications. *Progress in Polymer Science*, 85, 1-56.

Authors' information

Electric, Electronics and Computer Engineering Department, University of Catania. Viale A. Doria, 6 – 95125 Catania, Italy.

Edoardo Seminara received the Bachelors Degree in Industrial Engineering in 2022 from University of Catania. He currently is student at Federico II University Naples.

Giuseppe Laudani received the Bachelors Degree in Industrial Engineering in 2017 from University of Catania and the Master Degree in Mechanical Engineering in 2019 from University of Catania, Italy. He is currently an Engineering Researcher with Electric, Electronics and Computer Engineering Department at University of Catania. His research interests include Reverse Engineering techniques, Rapid Prototyping techniques, CAD-CAE Modeling, Algorithms, Computer Aided Tolerancing (CAT), Structural Optimization particularly in mechanical field.
E-mail: giuseppe.laudani@unict.it

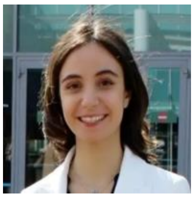

Giuliana Baiamonte received the Bachelors Degree in Industrial Engineering in 2019 from University of Catania and the Master Degree in Biomedical Engineering in 2022 at the BioMedical Campus in Rome, Italy. During her job training, she worked for the company Edwards Lifesciences in operating room in order to train the medical team (anesthetists and nurses) on the correct use of devices for hemodynamic monitoring in the perioperative. Her interests include devices based on nanotechnology and research to improve life.
E-mail: giuliana.baiamonte@unict.it

Michele Calì received the B.S. degree in Mechanical Engineering and Ph.D. degree in Engineering Structural Mechanics from University of Catania, Italy, in 1996 and 2000, respectively. He is currently an Engineering Professor at the Electric, Electronics and Computer Engineering Department -University of Catania-. He has published more than 90 articles in national and international journals and more than 50 papers in national and international conferences. His research interests include Reverse Engineering techniques, Rapid Prototyping techniques, CAD-CAE Method, Processing and modeling Algorithms, Computer Aided Tolerancing (CAT), Geometric and Structural Optimization in mechanical and biomedical field.
E-mail: michele.cali@unict.it